

Charged pion photoproduction from ^{10}B

D. Rowley,* J. LeRose,[†] K. Min, B. O. Sapp, P. Stoler, E. J. Winhold, and P. F. Yergin
Department of Physics, Rensselaer Polytechnic Institute, Troy, New York 12181

A. M. Bernstein, K. I. Blomqvist, H. S. Caplan,[‡] S. A. Dytman, G. Franklin,[§] and M. Pauli^{||}
*Laboratory for Nuclear Science, Massachusetts Institute of Technology,
 Cambridge, Massachusetts 02139*

(Received 26 October 1981)

Measurements were made of $d\sigma/d\Omega$ [$\theta_\pi=90^\circ(\text{lab})$] for $^{10}\text{B}(\gamma,\pi^+)^{10}\text{Be}$ (g.s.) at $T_\pi=17$, 29, and 42 MeV, for $^{10}\text{B}(\gamma,\pi^+)^{10}\text{Be}$ ($E_x=3.37$ MeV) at $T_\pi=29$ and 42 MeV, and for $^{10}\text{B}(\gamma,\pi^-)^{10}\text{C}$ (g.s.) at $T_\pi=29$ MeV. The results disagree significantly with several recent distorted-wave impulse approximation calculations.

[NUCLEAR REACTIONS $^{10}\text{B}(\gamma,\pi^+)^{10}\text{Be}$ ($E_x=0, 3.37$ MeV),
 $^{10}\text{B}(\gamma,\pi^-)^{10}\text{C}$ ($E_x=0$), $\theta_\pi=90^\circ$ (lab), $E_\pi=17, 29, 42$ MeV, measured
 $d\sigma/d\Omega$, compared with DWIA calculations.]

I. INTRODUCTION

There has been considerable interest in experimental studies of charged photopion production in complex nuclei in the past several years because of the possibility of their yielding information on the photoproduction amplitude in nuclei, on the nuclear structure of the states involved, and on the pion-nucleus interaction. These (γ,π^\pm) studies have particular potential as a nuclear structure probe because of their isospin selectivity, their preferential excitation of spin-flip transitions, and more particularly their strong excitation of isospin analogs of giant multipole resonances in the target nucleus.

Before such applications of (γ,π) reactions can be made with confidence, however, the validity of theoretical treatments of these reactions needs to be carefully checked. Current treatments are based on distorted wave impulse approximation (DWIA). These calculations typically employ one of several approximately equivalent formulations of the elementary photoproduction amplitude,¹⁻³ use nuclear wave function information which is derived from or tested against electron scattering data, and describe the pion-nucleus interaction in terms of an optical model treatment whose parameters are constrained by pion scattering data.

Such DWIA calculations have been compared to the limited amount of experimental data currently

available on (γ,π^\pm) differential cross sections to discrete final states. These data generally apply to pion energies less than 50 MeV (where the pion-nucleus interaction is weak) and to p -shell nuclei, where the nuclear structure information is generally known (with some notable exceptions). The results of such comparisons are somewhat mixed, though in most cases agreement between experiment and theory is to better than a factor of 2. Total cross sections for $^{12}\text{C}(\gamma,\pi^-)^{12}\text{N}$ (g.s.) and $^7\text{Li}(\gamma,\pi^-)^7\text{Be}$ (g.s.) measured from threshold to 360 MeV photon energy^{4,5} are well fit by DWIA calculations using both shell model⁶ and Helm model⁷ matrix elements. Differential cross sections for $^{12}\text{C}(\gamma,\pi^+)^{12}\text{B}$ (g.s.) from Tohoku at 194 MeV ($T_\pi \simeq 39$ MeV) and for this reaction and $^{12}\text{C}(\gamma,\pi^-)^{12}\text{N}$ (g.s.) from Bates at 17 and 29 MeV pion energies⁹ are all in fair agreement (factor of 2 or less) with shell¹⁰ and Helm⁷ model calculations. On the other hand, $^{12}\text{C}(\gamma,\pi^+)^{12}\text{B}$ ($E_x=0.95$ MeV) data from Tohoku⁸ and Bates⁹ are lower than the calculation of Singham and Tabakin¹⁰ by a factor of about 3, but are in fair agreement with the calculation of Nagl and Überall.⁷ For $^{12}\text{C}(\gamma,\pi^+)$ leading to the 4.5 MeV complex in ^{12}B , there is good agreement with shell and Helm model calculations consistent with (e,e') data.¹¹ For $^6\text{Li}(\gamma,\pi^+)^6\text{He}$ (g.s.) there is good agreement between experiment and theory both for the near threshold total cross sec-

tion¹² and for differential cross sections at photon energies up to 195 MeV, corresponding to momentum transfer values up to 200 MeV/c.¹³ However, there are factor of 2 discrepancies between experiment and theory for $^6\text{Li}(\gamma, \pi^+)$ leading to the first excited state of ^6He .¹³ For $^{16}\text{O}(\gamma, \pi^+)$ leading to the low-lying levels in ^{16}N , calculated differential cross sections^{14,15} at 200 MeV photon energy differ from experiment¹⁶ by factors of between 2 and 3 although this case is complicated because it involves the unresolved sum of transitions to four states in ^{16}N .

$^{10}\text{B}(\gamma, \pi^\pm)$ is an attractive choice as an additional test case for several reasons. As can be seen from the level diagram of Fig. 1, the ground and first excited states of the residual nuclei ^{10}Be and ^{10}C are readily resolved. The nuclear structure appears to be well in hand. The Cohen-Kurath intermediate coupling wave functions¹⁷ fit (e, e') scattering¹⁸ data to the analog states in ^{10}B quite well, showing that the relevant states are predominantly p -shell states. The transition to the 1.74 MeV 0^+ state in ^{10}B (analog of ^{10}Be ground state) is pure $M3$ and the transition to the 5.17 MeV 2^+ state in ^{10}B (analog of ^{10}Be and ^{10}C first excited states) is predominantly $M3$, and we expect both (e, e') and (γ, π) to these states to be dominated by spin-flip transitions. The present experiment covers a range of momentum transfer which places it well up on the first maximum of the form factor where pion counting rates should be relatively high and the cross sections should be rather insensitive to second-order effects. Finally, ^{10}B is self-conjugate, so that (γ, π^+) and (γ, π^-) lead to corresponding $T=1$ analog states in ^{10}Be and ^{10}C , and isospin effects may be investigat-

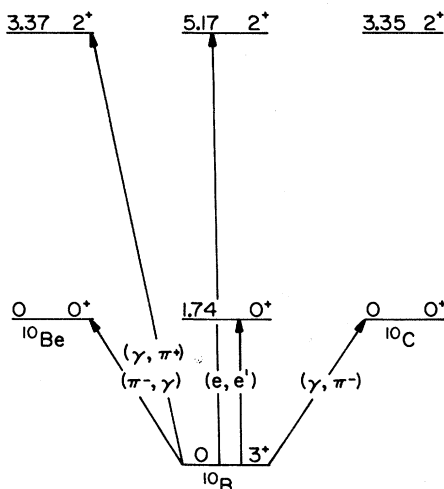


FIG. 1. Relevant $A=10$ energy levels. Only the $T=0$ ^{10}B ground state and the lowest $T=1$ levels are shown.

ed by comparing (γ, π^+) and (γ, π^-) results.

In the present experiment we have measured differential cross sections at $\theta_\pi(\text{lab})=90^\circ$ for $^{10}\text{B}(\gamma, \pi^+)^{10}\text{Be}$ ($E_x=0, 3.37$ MeV) at 17, 29, and 42 MeV pion energies, and for $^{10}\text{B}(\gamma, \pi^-)^{10}\text{C}$ ($E_x=0$) at $T_\pi=29$ MeV. Concurrently, positive photopion angular distribution measurements on ^{10}B at a single photon energy have been made by Yamazaki²⁰ at Tohoku. These latter measurements complement the present results, which are confined to a single pion angle, but which cover several pion energies.

II. EXPERIMENT

The experimental layout is shown in Fig. 2. The electron beam from the Bates linac passed through flux and position monitors and traversed a tungsten bremsstrahlung radiator of thickness 186 mg/cm². The mixed photon-electron beam then passed through the ^{10}B target located about 5 cm downstream from the radiator. Targets were constructed by pressing isotopically-enriched (86% ^{10}B) boron powder into discs of 2.2 cm diameter and intrinsic thickness about 100 mg/cm², and were mounted at 45° to the incident beam. Pions emerging from the target at 90° were momentum analyzed in a quadrupole-dipole magnetic spectrometer system which is described in detail elsewhere.²¹ A multiwire proportional counter was located in the focal plane followed by an array of three scintillation counters and one Cerenkov counter used for particle identification.

Data were taken at pion energies of about 17, 29, and 42 MeV. At each pion energy the spectrometer setting was held constant, and wire chamber spectra were acquired at each of a series of electron energies spaced 1 to 3 MeV apart. Data were periodically taken at an electron energy of 230 MeV, where the

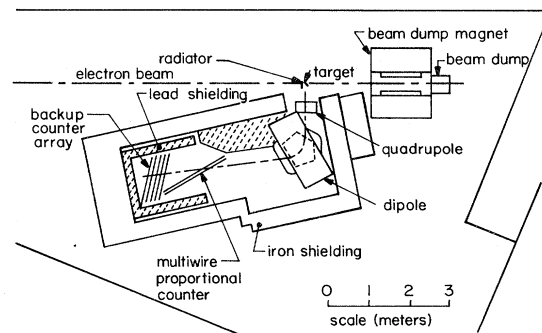


FIG. 2. Experimental layout.

pion spectrum was relatively smooth and flat, to check the relative channel-by-channel efficiency of the wire chamber. In order to enable subtraction of the contribution of the ^{11}B target contaminant in the $^{10}\text{B}(\gamma, \pi^-)$ experiment, (γ, π^-) data were also taken with a ^{11}B target. Because of threshold energy differences, there was no ^{11}B contribution to the (γ, π^+) data. All data were recorded on magnetic tape in an event-by-event mode.

In order to fix the absolute cross section scale, a set of hydrogen normalization runs was made at 230 and 245 MeV using a 54 mg/cm² polyethylene target. The pion yield from hydrogen dominates in these runs; similar runs were made with a graphite target to permit subtraction of the carbon contribution to the yield.

III. DATA REDUCTION AND ANALYSIS

Acceptable events were selected by sorting on the basis of acceptable wire chamber firing and cuts in pulse heights and time-of-flight spectra in the three scintillators, and the Cerenkov time-of-flight spectrum.^{21,22} Effects of channel-by-channel efficiency variations were removed by dividing the wire chamber spectrum of acceptable events by that obtained at an electron energy of 230 MeV with the same spectrometer setting. Then the resulting wire chamber spectra for various electron energies at a particular spectrometer setting were combined into a single isochromat plot (number of pions per unit energy versus electron energy for a particular pion kinetic energy). This method of obtaining isochromats is described in detail elsewhere.²² The plot for $T_\pi = 29$ MeV is shown in Fig. 3.

Cross sections were extracted by fitting the isochromats constructed in this way with a standard photon spectrum. This photon spectrum included bremsstrahlung from radiator and target using a code of Matthews and Owens,²³ and a virtual spectrum for electroproduction as given by Dalitz and Yennie²⁴ with an experimentally-determined correction factor of 1.25.²⁵ Electron and pion energy losses in radiator and target were accounted for in the photon spectrum as was the system energy resolution. Real bremsstrahlung photons contributed about two-thirds of the pion yield in the present experiment and virtual photons about one third. In obtaining cross sections, pion decay was taken into account, but the muon contamination of the pion spectra (estimated to be a few percent) was neglected. No correction was made for contributions to

the background from quasifree processes. Absolute cross sections were determined relative to that of $^1\text{H}(\gamma, \pi^+)$, using the cross section tabulation of Genzel *et al.*²⁶ for that reaction.

IV. RESULTS AND DISCUSSION

The cross section values obtained for $^{10}\text{B}(\gamma, \pi^+)^{10}\text{Be}(\text{g.s.})$ at $T_\pi = 17, 29$, and 42 MeV are plotted in Fig. 4 and those of the corresponding reaction leading to the first excited state of ^{10}Be ($E_x = 3.37$ MeV) at $T_\pi = 29$ and 42 MeV are plotted in Fig. 5. The error bars shown include only statistical errors. In addition, the absolute cross section scale is uncertain by about $\pm 16\%$ owing to the combined effect of systematic errors, including uncertainties in target thickness, $^1\text{H}(\gamma, \pi^+)$ absolute cross section, and real and virtual photon spectra. Recent measurements by Yamazaki²⁰ at $T_\pi = 40$ MeV are also shown in these figures. There is satis-

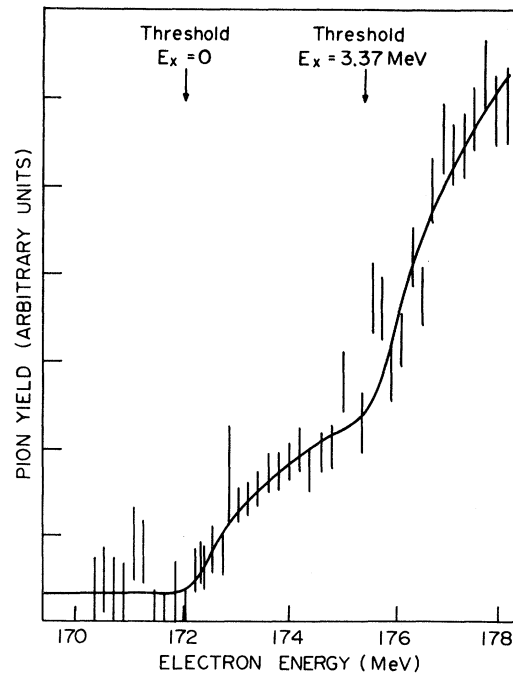


FIG. 3. Yield of positive pions with $T_\pi = 29$ MeV from ^{10}B as a function of electron energy, as constructed from the experimental data. The vertical bars on the data points represent statistical errors. The solid curve is a least-squares fit to the data which includes a flat background contribution and above-threshold contributions from the transitions to the ground and 3.37 MeV states of ^{10}Be . The shapes of each of the latter contributions reflect calculated photon spectrum shapes as described in the text.

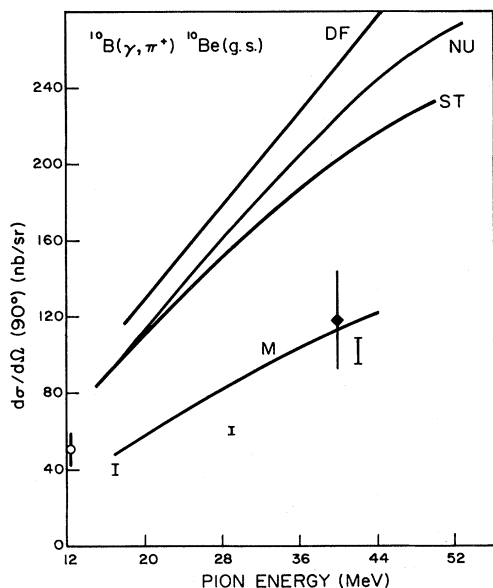


FIG. 4. Differential cross sections for $^{10}\text{B}(\gamma, \pi^+)^{10}\text{Be}$ (ground state) at $\theta_\pi = 90^\circ$ (lab). The present results are given by the vertical bars. Other experimental results are shown as the solid diamond point at 40 MeV (Ref. 20) and the open circle point near 12 MeV (deduced from Ref. 27). The curves labeled *M* (Ref. 31), *ST* (Ref. 10), *DF* (Ref. 30), and *NU* (Ref. 28) are the results of the four different theoretical calculations as described in the text.

factory agreement between his results and the present data. Also shown in Fig. 4 is a result for the (γ, π^+) ground state cross section at $T_\pi = 12.3$ MeV which we deduced from the $^{10}\text{B}(e, \pi^+)$ cross section, obtained in a recent measurement at Saskatchewan,²⁷ through use of the Dalitz-Yennie virtual photon spectrum²⁴ with an experimentally determined correction factor of 1.25.²⁵ This result and the present results appear to be consistent within their sizable combined errors. The cross section obtained in the present work for $^{10}\text{B}(\gamma, \pi^-)^{10}\text{C}(\text{g.s.})$ at $T_\pi = 29$ MeV is given in Fig. 6. Measured cross section values are listed in Table I.

The results of four independent DWIA calculations are also shown in Figs. 4–6. We have calculated cross sections using a code by Nagl and Überall²⁸ (*NU*) which is based on the Helm model, uses the elementary amplitude of Berends *et al.*,² and includes pion distortion via a second order optical potential. The calculation of Singham and Tabakin¹⁰ (*ST*) uses the Blomqvist-Laget³ form for the elementary amplitude, and employs the nuclear wave functions of Cohen and Kurath¹⁷ with the pion optical potential of Stricker *et al.*²⁹ DeCarlo and Freed³⁰ (*DF*) have also made a calculation simi-

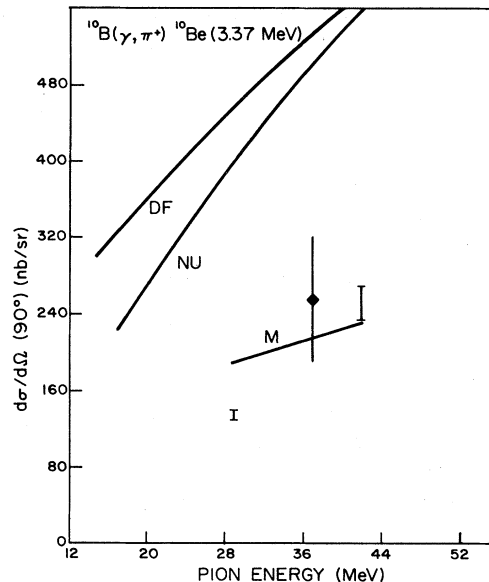


FIG. 5. Results for $^{10}\text{B}(\gamma, \pi^+)^{10}\text{Be}$ ($E_x = 3.37$ MeV) at $\theta_\pi = 90^\circ$ (lab). See caption for Fig. 4.

lar to *ST*, except that they use the elementary amplitude of Berends *et al.*² The calculation of Maleki³¹ (*M*) uses the elementary amplitude of Chew *et al.*,¹ and Cohen-Kurath wave functions, but uses a first-order pion optical potential of the local Laplacian form. Maleki's calculation agrees with the data to within $\approx 40\%$ for all points, while the *NU*, *ST*, and *DF* results are higher than the

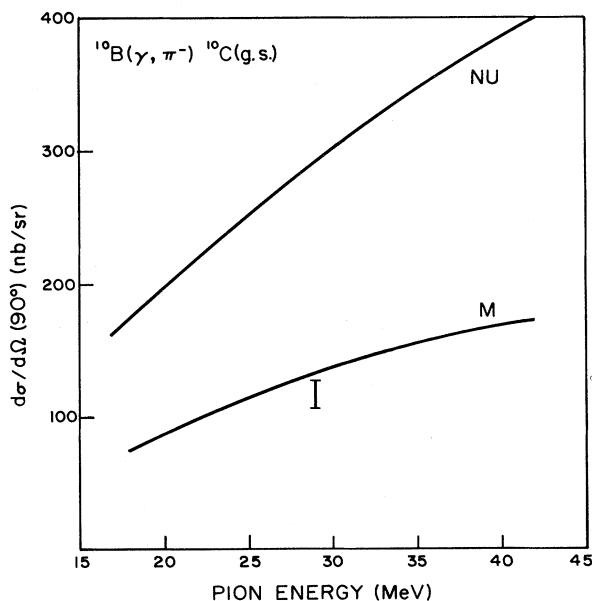


FIG. 6. Results for $^{10}\text{B}(\gamma, \pi^-)^{10}\text{C}$ (ground state) at $\theta_\pi = 90^\circ$ (lab). See caption for Fig. 4.

TABLE I. Experimental differential cross section results (in nb/sr) for $^{10}\text{B}(\gamma, \pi)$ at $\theta_\pi=90^\circ$ (lab). The uncertainties quoted for the present results are statistical only (see text).

	$\frac{d\sigma}{d\Omega}(\gamma, \pi^+) \text{ (g.s.)}$			$\frac{d\sigma}{d\Omega}(\gamma, \pi^+)(E_x=3.37 \text{ MeV})$		$\frac{d\sigma}{d\Omega}(\gamma, \pi^-)(\text{g.s.})$
	$T_\pi=17 \text{ MeV}$	$T_\pi=29 \text{ MeV}$	$T_\pi=42 \text{ MeV}$	$T_\pi=29 \text{ MeV}$	$T_\pi=42 \text{ MeV}$	$T_\pi=29 \text{ MeV}$
Present Results	41 ± 3	62 ± 2	104 ± 7	136 ± 4	254 ± 13	117 ± 10
Yamazaki ^a ($T_\pi \simeq 40 \text{ MeV}$)			117 ± 27		256 ± 65	

^aReference 20.

data by a factor of between 2 and 3. These calculations are more complete than Maleki's in that they include second-order terms in the pion optical potential, but in the pion energy range of the experiment these terms should not be important enough to account for the cross section differences. We note that the significant discrepancy between the present data and the NU, ST, and DF results occurs for $^{10}\text{B}(\gamma, \pi^+)$ leading to both the ground and first excited states of ^{10}Be , as well as for $^{10}\text{B}(\gamma, \pi^-)^{10}\text{C}(\text{g.s.})$. Table II lists the measured and calculated values of the $(\gamma, \pi^-)/(\gamma, \pi^+)$ cross section ratio for the ground state transition at 29 MeV; we find agreement to $\simeq 20\%$ for this ratio which we expect to be effectively independent of the nuclear wave functions. It appears unlikely that the assumptions made in the calculation with regard to the elementary amplitude and pion final state interactions can be markedly invalid. The effect of pion distortion for $^{10}\text{B}(\gamma, \pi^+)^{10}\text{Be}(\text{g.s.})$ can be seen

in Fig. 7 which shows the NU results for both plane wave pions and fully distorted pions. Below 190 MeV, in the energy region of this experiment, the effect of distortion is less than 30%. Thus we are led to particularly examine the nuclear structure input to the calculations. The Cohen-Kurath wave functions used in the ST, DF, and Maleki calculations contain only p -shell configurations but have been tested against inelastic electron scattering data to the analog states at 1.74 and 5.17 MeV in ^{10}B .¹⁸ The agreement is quite satisfactory over the momentum transfer range covered ($0.7-1.8 \text{ fm}^{-1}$); this includes the range appropriate to the present experiment. The NU Helm model calculation obtains its nuclear structure input by a direct parametrization of electron scattering data. This procedure is not completely unambiguous, however. As can be seen in Table II, both the NU and Maleki calculations do a reasonable job of calculating the ratio of the cross sections for (γ, π^+) leading to the

TABLE II. $^{10}\text{B}(\gamma, \pi)$ differential cross section ratios at $\theta_\pi=90^\circ$ (lab).

	$\frac{d\sigma}{d\Omega}(\gamma, \pi^+)(E_x=3.37\text{MeV})$		$\frac{d\sigma}{d\Omega}(\gamma, \pi^-) \text{ (g.s.)}$
	$T_\pi=29 \text{ MeV}$	$T_\pi=42 \text{ MeV}$	$\frac{d\sigma}{d\Omega}(\gamma, \pi^+) \text{ (g.s.)}$ $T_\pi=29 \text{ MeV}$
Experiment:			
Present results	2.19 ± 0.11	2.44 ± 0.21	1.89 ± 0.18
Yamazaki ^a ($T_\pi \simeq 40 \text{ MeV}$)		2.19 ± 0.75	
Theory:			
Nagl-Überall code ^b (NU)	2.44	2.38	1.80
Maleki ^c (M)	2.16	1.96	1.55
DeCarlo-Freed ^d (DF)	2.45	2.16	

^aReference 20.

^bReference 28.

^cReference 31.

^dReference 30.

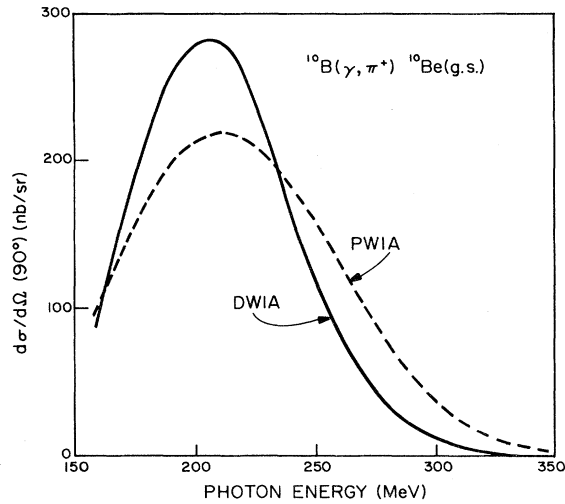


FIG. 7. Differential cross section for $^{10}\text{B}(\gamma, \pi^+)^{10}\text{Be}(\text{g.s.})$ at 90° as calculated using the Helm model code of fully-distorted pions (DWIA).

ground and first excited states of ^{10}Be . Figure 8 shows that this measured ratio also appears to be consistent with (π^-, γ) (Refs. 32 and 33) and (e, e') (Ref. 18) data, and (γ, π) data taken at higher momentum transfer.³⁴ We conclude that any major errors in the treatment of nuclear structure in the calculations must be common to both ground and first excited state transitions.

One special feature of the ^{10}B transitions is that they are either pure $M3$ (ground state transition) or predominantly $M3$ (first excited state transition). This should in fact make for a simple situation in ^{10}B , since as Bergstrom¹⁹ has shown, $M3$ transition between pure p -shell configurations should involve only a spin current contribution, with the convection current vanishing. Thus the (e, e') transition density used in the Helm calculation should be quite appropriate for the (γ, π) case, to the extent that it is

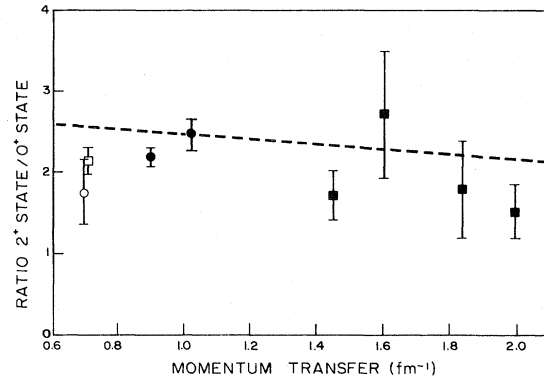


FIG. 8. Ratio of $^{10}\text{B}(\gamma, \pi^+)$ differential cross sections to the 2^+ 3.37 MeV and 0^+ states of ^{10}Be as a function of momentum transfer. The solid circles are the present results and the solid squares are the results of Bosted *et al.* (Ref. 34). Also shown is the form factor ratio for the analogs of these two states in ^{10}B obtained from (e, e') (Ref. 18), and the ratio of $^{10}\text{B}(\gamma, \pi^-, \gamma)$ branching ratios for the two states (open circle: Ref. 33; open square: Ref. 32).

dominated by the $\vec{\sigma} \cdot \vec{\epsilon}$ term in the photoproduction operator. However, there are differences between (e, e') and (γ, π) calculations. Although most of the (γ, π) cross section for $T_\pi < 50$ MeV is due to the $\vec{\sigma} \cdot \vec{\epsilon}$ operator, which is identical to the (e, e') magnetic spin transition operation, the remaining terms in the operator are more complicated.

It is of interest to examine the experimental and theoretical results on the closely-related radiative pion capture reaction $^{10}\text{B}(\pi^-, \gamma)$ connecting the same states as (γ, π^+) . This process occurs at a fixed momentum transfer ($q \simeq 0.7 \text{ fm}^{-1}$) somewhat lower than the range of q covered by the present (γ, π^+) experiment. Table III summarizes the values obtained for the branching ratio in experiments at Berkeley³³ and Schweizerisches Institut für Nuklearforschung³² and in two independent im-

TABLE III. $^{10}\text{B}(\pi^-, \gamma)^{10}\text{Be}$ branching ratios for transitions to the lowest two states of ^{10}Be . The uncertainties in the theoretical values reflect the uncertainties in the pionic x-ray data used.

^{10}Be final state	Experiment $\times 10^4$		Theory $\times 10^4$	
	Baer <i>et al.</i> ^a	Alder <i>et al.</i> ^b	Baer <i>et al.</i> ^a	Dogotar <i>et al.</i> ^c
0^+ ground state	2.5 ± 0.4	2.31 ± 0.15	3.6 ± 0.7	2.3 ± 0.5
2^+ 3.37 MeV	4.4 ± 0.7	4.88 ± 0.2	8.5 ± 1.7	5.7 ± 1.1

^a Reference 33.

^b Reference 32.

^c Reference 35.

pulse approximation calculations.^{33,35} It can be seen that the results of the two experiments and the calculation of Dogotar *et al.*³⁵ are all in good agreement but the results of the calculation of Baer *et al.*³³ are higher. The differences in branching ratio values from the two calculations primarily reflect differences in the calculated values for the basic transition rates, especially the dominant capture rate from the $2p$ orbit. These calculated rate differences probably reflect differences in the wave functions used. We note that Dogotar *et al.* use Cohen-Kurath wave functions,¹⁷ which are in good agreement with (e,e') form factor data.¹⁸ The wave functions used by Baer *et al.* are also p -shell intermediate coupling wave functions, but they have not been tested against (e,e') data.

Finally, we point out that all four calculations for the $^{10}\text{B}(\gamma,\pi^+)^{10}\text{Be}(\text{g.s.})$ ground state transition have been extended up to a photon energy of about 340 MeV and compared to the higher energy data of Bosted *et al.*³⁴ (Fig. 9). There are major discrepancies among the calculations, but all four show a broad peak centered near 200 MeV. The low energy rise and peak region reflects nuclear structure factors as contained to some extent in the $M3$ factor. However the peak is shifted by some 30 MeV from the place where the form factor peaks. The pion final state interactions are relatively weak in this energy region and the energy dependence of the elementary amplitude is not so important. The falloff at higher energies reflects the form factor falloff, strongly accentuated by pion interactions. The cross section here is particularly sensitive to the situation at the nuclear surface and to the pion-nucleus interaction, and relatively insensitive to the nuclear wave functions in the nuclear interior. All four calculations disagree in the peak region. The DF and ST calculations are consistent with the high energy data, but NU and M are not. It is not clear what differences in the calculations give rise to these differences.

To summarize our results, the present experiment is in agreement with independent measurements at $T_\pi=12$ and 40 MeV, but there are significant discrepancies between experiment and the NU, ST, and DF calculations and among the several calculations. The reasons for these surprising discrepancies in this important test case for the (γ,π) reaction are not yet evident. Certainly the DWIA theory should be constrained well for this case, with weak pion distortions and the nuclear structure information well determined. In fact, three of the four calculations use the same nuclear structure input and

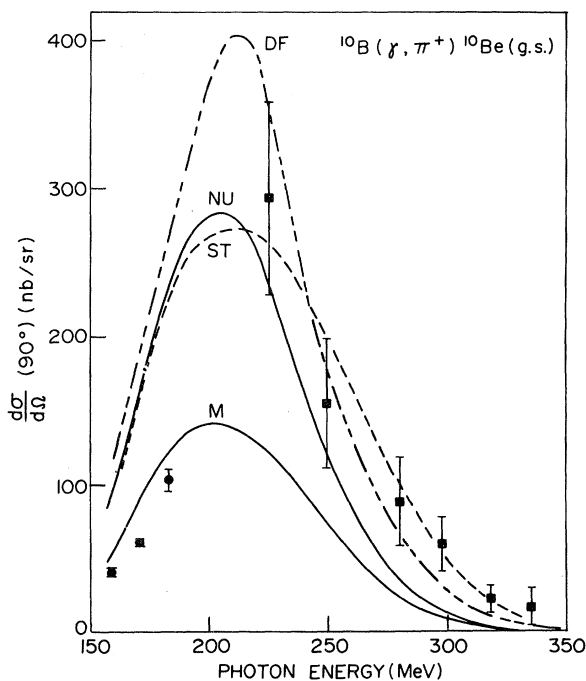


FIG. 9. Differential cross section at 90° for $^{10}\text{B}(\gamma,\pi^+)^{10}\text{Be}(\text{g.s.})$ at photon energies up to 340 MeV. The solid circles are the present results and the solid squares are the higher energy results of Bosted *et al.* (Ref. 34). The curves are the results of four different theoretical calculations as described in the text.

all four use structure information which fits the (e,e') data. Certainly further theoretical work is needed and is in fact in progress. In any case we plan further experimental work on ^{10}B which will include angular distribution measurements over a wider range of pion energies.

ACKNOWLEDGMENTS

We thank A. Nagl and H. Überall for allowing us to use their Helm model program, B. N. Sung for assisting with the data taking, M. K. Singham, F. Tabakin, N. Freed, V. DeCarlo, and S. Maleki for communicating the results of their calculations prior to publication, and the Bates Laboratory staff for their helpfulness during the experiment. This work was supported by National Science Foundation Grants PHY77-09408 and PHY80-06954 and by Department of Energy Contract No. EY-76-C-02-3069.

- *Present address: Lawrence Livermore National Laboratory, Livermore, California 94550.
- †Present address: Department of Physics, Louisiana State University, Baton Rouge, Louisiana 70803.
- ‡On leave from University of Saskatchewan, Saskatoon, Saskatchewan, Canada.
- §Present address: Department of Physics, Carnegie-Mellon University, Pittsburgh, Pennsylvania 15213.
- ||Present address: General Research Corporation, 7655 Old Springhouse Rd., Westgate Research Park, McLean, Virginia 22102.
- ¹G. F. Chew, M. L. Goldberger, F. E. Low, and Y. Nambu, *Phys. Rev.* **106**, 1345 (1957).
- ²F. A. Berends, A. Donnachie, and D. L. Weaver, *Nucl. Phys.* **B4**, 1 (1967).
- ³I. Blomqvist and J. M. Laget, *Nucl. Phys.* **A280**, 405 (1977).
- ⁴A. M. Bernstein *et al.*, *Phys. Rev. Lett.* **37**, 819 (1976).
- ⁵P. E. Bosted, K. I. Blomqvist, and A. M. Bernstein, *Phys. Rev. Lett.* **43**, 1473 (1979).
- ⁶M. K. Singham, G. N. Epstein, and F. Tabakin, *Phys. Rev. Lett.* **43**, 1476 (1979).
- ⁷A. Nagl and H. Überall, *Phys. Lett.* **96B**, 254 (1980).
- ⁸K. Shoda, H. Ohashi, and K. Nakahara, *Phys. Rev. Lett.* **39**, 1131 (1977); *Nucl. Phys.* **A350**, 377 (1980).
- ⁹N. Paras *et al.*, *Phys. Rev. Lett.* **42**, 1455 (1979).
- ¹⁰M. Singham and F. Tabakin, *Ann. Phys. (N.Y.)* **135**, 71 (1981).
- ¹¹K. Min *et al.*, *Phys. Rev. Lett.* **44**, 1384 (1980).
- ¹²G. Audit *et al.*, *Phys. Rev. C* **15**, 1415 (1977); **20**, 242 (1979).
- ¹³K. Shoda, O. Sasaki, and T. Kohmura, *Phys. Lett.* **101B**, 124 (1981).
- ¹⁴A. Nagl and H. Überall, *Photopion Nuclear Physics*, edited by P. Stoler (Plenum, New York, 1979), p. 155.
- ¹⁵R. D. Graves *et al.*, *Can. J. Phys.* **58**, 48 (1980).
- ¹⁶H. Ohashi *et al.*, *Photopion Nuclear Physics*, edited by P. Stoler (Plenum, New York, 1979), p. 193.
- ¹⁷S. Cohen and D. Kurath, *Nucl. Phys.* **73**, 1 (1965).
- ¹⁸E. J. Ansaldò, J. C. Bergstrom, R. Yen, and H. S. Caplan, *Nucl. Phys.* **A322**, 237 (1979).
- ¹⁹J. C. Bergstrom, *Phys. Rev. C* **21**, 2496 (1980).
- ²⁰M. Yamazaki, Ph.D. thesis, Tohoku University, 1981 (unpublished).
- ²¹N. Paras *et al.*, *Nucl. Instrum. Methods* **167**, 215 (1979).
- ²²D. Rowley, Ph.D. thesis, Rensselaer Polytechnic Institute, 1981 (unpublished); P. Stoler *et al.* (unpublished).
- ²³J. L. Matthews and R. O. Owens, *Nucl. Instrum. Methods* **111**, 157 (1973).
- ²⁴R. H. Dalitz and D. R. Yennie, *Phys. Rev.* **105**, 1598 (1957).
- ²⁵P. Stoler *et al.*, *Phys. Rev. C* **22**, 911 (1980).
- ²⁶H. Genzel, P. Joos, and W. Pfeil, *Landolt-Börnstein, Zahlenwerte und Funktionen aus Naturwissenschaften und Technik* (Springer, Berlin, 1973), Vol. 8.
- ²⁷H. S. Caplan (private communication).
- ²⁸A. Nagl and H. Überall (private communication).
- ²⁹K. Stricker, H. McManus, and J. A. Carr, *Phys. Rev. C* **19**, 929 (1979).
- ³⁰V. DeCarlo and N. Freed (private communication).
- ³¹S. Maleki, Ph. D. thesis, Rensselaer Polytechnic Institute, 1981 (unpublished).
- ³²J. C. Alder *et al.*, *Photopion Nuclear Physics*, edited by P. Stoler (Plenum, New York, 1979), p. 101.
- ³³H. W. Baer *et al.*, *Phys. Rev. C* **12**, 921 (1975).
- ³⁴P. E. Bosted *et al.*, *Phys. Rev. Lett.* **45**, 1544 (1980); P. E. Bosted, Ph.D. thesis, Massachusetts Institute of Technology, 1980.
- ³⁵G. E. Dogotar, R. A. Eramzhyan, H. R. Kissener, and R. A. Sakaev, *Nucl. Phys.* **A282**, 474 (1977).